

PRR11 unveiled as a top candidate biomarker within the RBM3-regulated transcriptome in pancreatic cancer

Sofie Olsson Hau^{1*} , Sara Wahlin¹, Sophie Cervin¹, Vilgot Falk¹, Björn Nodin¹, Jacob Elebro¹, Jakob Eberhard¹, Bruce Moran², William M Gallagher², Emelie Kamevi¹ and Karin Jirström¹

¹Division of Oncology and Therapeutic Pathology, Department of Clinical Sciences, Lund University, Lund, Sweden

²UCD School of Biomolecular and Biomedical Science, UCD Conway Institute, University College Dublin, Dublin, Ireland

*Correspondence to: Sofie Olsson Hau, Division of Oncology and Therapeutic Pathology, Department of Clinical Sciences, Lund University, Lund, Sweden. E-mail: sofie.olsson_hau@med.lu.se

Abstract

The outlook for patients with pancreatic cancer remains dismal. Treatment options are limited and chemotherapy remains standard of care, leading to only modest survival benefits. Hence, there is a great need to further explore the mechanistic basis for the intrinsic therapeutic resistance of this disease, and to identify novel predictive biomarkers. RNA-binding motif protein 3 (RBM3) has emerged as a promising biomarker of disease severity and chemotherapy response in several types of cancer, including pancreatic cancer. The aim of this study was to unearth RBM3-regulated genes and proteins in pancreatic cancer cells *in vitro*, and to examine their expression and prognostic significance in human tumours. Next-generation RNA sequencing was applied to compare transcriptomes of MIAPaCa-2 cells with and without RBM3 knockdown. The prognostic value of differentially expressed genes (DEGs) was examined in The Cancer Genome Atlas (TCGA). Top deregulated genes were selected for further studies *in vitro* and for immunohistochemical analysis of corresponding protein expression in tumours from a clinically well-annotated consecutive cohort of 46 patients with resected pancreatic cancer. In total, 19 DEGs ($p < 0.01$) were revealed, among which some with functions in cell cycle and cell division stood out; *PDS5A* (PDS cohesin associated factor A) as the top downregulated gene, *CCND3* (cyclin D3) as the top upregulated gene, and *PRR11* (proline rich 11) as being highly prognostic in TCGA. Silencing of RBM3 in MiaPaCa-2 cells led to congruent alterations of *PDS5A*, cyclin D3, and *PRR11* levels. High protein expression of *PRR11* was associated with adverse clinicopathological features and shorter overall survival. Neither *PDS5A* nor cyclin D3 protein expression was prognostic. This study unveils several RBM3-regulated genes with potential clinical relevance in pancreatic cancer, among which *PRR11* shows the most consistent association with disease severity, at both transcriptome and protein levels.

Keywords: cyclin D3; pancreatic cancer; *PDS5A*; prognosis; *PRR11*; RBM3-regulated genes

Received 9 April 2021; Revised 7 June 2021; Accepted 12 July 2021

No conflicts of interest were declared.

Introduction

Pancreatic cancer is a grievous disease, and the outlook for afflicted patients remains dismal with an estimated 5-year survival of less than 10% [1]. It is the most common tumour among a heterogeneous group of neoplasms arising in the periampullary region, including tumours originating in the distal bile duct, pancreas, ampulla of Vater, and the periampullary duodenum. Unlike many other cancers, targeted therapies including immune checkpoint inhibition have shown little efficacy against pancreatic cancer and, if so, only for a small

selection of patients [2–6]. Therefore, chemotherapy remains standard of care, leading to modest survival benefits [7]. Thus, there is a pressing need to identify novel complementary biomarkers to better distinguish patients who are likely to benefit from standard chemotherapy from those who will only suffer from negative side effects and thus fare better with other treatment approaches or best supportive care.

RNA-binding motif protein 3 (RBM3) is an RNA- and DNA-binding protein that has emerged as a promising independent predictive and prognostic biomarker in several solid tumours, including pancreatic cancer [8–

14]. In a previous study by our group, silencing of RBM3 was found to render pancreatic cancer cells less sensitive to a variety of chemotherapeutic agents *in vitro*. Furthermore, in patients with resected pancreatic and other periampullary cancers, high tumour-specific expression of RBM3 was found to be associated with prolonged overall survival (OS) if adjuvant treatment had been given, whereas the opposite was seen if no adjuvant treatment had been given [8]. Similar associations between RBM3 and sensitivity to cisplatin have been described in epithelial ovarian cancer [14], and further mechanistic clues may be derived from another study on ovarian cancer, demonstrating links between RBM3 and cellular processes such as chromatin remodelling, DNA integrity maintenance, and repair [15].

The aim of the present study was to explore RBM3-regulated genes and cellular processes that may influence the biological properties and chemosensitivity of pancreatic adenocarcinoma using RNA interference and next-generation RNA sequencing of transcriptomes *in vitro*. The top deregulated genes and proteins were further validated *in vitro* and explored regarding their expression, clinicopathological correlates, and prognostic significance in tumours from a clinically well-characterised cohort of patients with resected pancreatic adenocarcinoma ($n = 46$).

Materials and methods

Cell culture

Human pancreatic cancer cell lines BxPC-3, PANC-1, and MIAPaCa-2 were purchased from Sigma-Aldrich (St. Louis, MO, USA). The cells were maintained in RPMI1640 or DMEM supplemented with 10% foetal bovine serum (FBS) and antibiotics (100 U/ml penicillin and 100 µg/ml streptomycin) in a humidified 5% CO₂ atmosphere at 37 °C. All *in vitro* reagents, including cell culture medium and supplements, were purchased from ThermoFisher Scientific (Waltham, MA, USA) unless stated otherwise.

siRNA transfection

For siRNA transfection, pancreatic cancer cells were seeded in T-25 flasks ($4\text{--}7 \times 10^5$ cells) and incubated for 72 h at 37 °C. The cells were then washed twice with phosphate-buffered saline and received growth medium without FBS, together with lipofectamine 2000 and negative control or anti-RBM3 (s11858 + s11860) siRNA in OptiMEM to a final siRNA

concentration of 25 nM. The transfection was stopped after 4.5 h, medium was changed to full growth medium, and the cells were left to recover overnight. The following day, cells were harvested and spun down to pellets. The pellets were either fixated, dehydrated, and embedded in paraffin for immunohistochemistry or resuspended in TRIzol and stored at -20 °C for quantitative polymerase chain reaction (qPCR).

RNA sequencing

MIAPaCa-2 cells were transfected with siRNA targeting RBM3 or negative control, as described above, and RNA purification was performed in the same manner as for the qPCR samples. Samples were prepared in triplicate. RNA quantification and quality assessment were performed using Nanodrop 1000 (Mason Technology, Dublin, Ireland) and Bioanalyzer 2100 (Agilent, Santa Clara, CA, USA). cDNA libraries were prepared from the RNA samples using TruSeq Stranded mRNA Library Prep Kit on the NeoPrep instrument (Illumina, San Diego, CA, USA) according to the manufacturer's instructions, and sequenced (paired-end 1×75 bp) using the NextSeq 500 platform (Illumina). Fastq files were downloaded from the Illumina BaseSpace using the BaseSpace download tool and the quality of the files was determined using FastQC. Data were trimmed of sequencing adaptors and low-quality base calls using BBDuk tool in the BBMap package. Alignment to the human hg19/GRCh37 genome reference was done using STAR version 2.5.2a [16]. Duplicate reads were marked using Picard MarkDuplicates. Read counts were produced by the featureCounts tool from the SubRead package, combined for all samples and used as input for analysis of differential gene expression. Differential expression (DE) gene analysis was conducted using the R package DESeq2 [17] and genes with adjusted P value of <0.01 were selected for further analyses. The data set is deposited at the NCBI Gene Expression Omnibus database (GSE169758).

Real-time qPCR

The cell samples were thawed and RNA purification was performed using TRIzol with phasemaker tubes according to the manufacturer's instructions. Following this, RNA clean-up was performed with the RNeasy MinElute Cleanup Kit (QIAGEN, Hilden, Germany) and the RNA concentration was determined using Qubit with the RNA HS Assay Kit. Prior to qPCR, cDNA reverse transcription was performed

using the High-Capacity cDNA Reverse Transcription Kit and total cDNA concentration was determined using Qubit with the DNA Assay Kit. Ten ng per reaction of each samples was used to run qPCR with RBM3, PDS5A, PRR11, or CCND3 TaqMan gene expression assay (Assay ID Hs00943160_g1, Hs00374857_m1, Hs00383634_m1, or Hs05046059_s1, respectively), with samples run in triplicates. GAPDH was used as endogenous control (Assay ID Hs03929097_g1).

Western immunoblotting

Cells were seeded in 6-well plates (2×10^5) and incubated for 48 h at 37 °C prior to siRNA transfection. The day after transfection, cells were washed, lysed, and stored at -20 °C. Protein determination was performed with Pierce BCA protein assay and 20 µg was used from each sample. Samples were denatured in Laemmli sample buffer (Sigma-Aldrich) and boiled for 5 min at 95 °C. The samples were placed on a 8–16% TGX gradient gel (Bio-Rad, Hercules, CA, USA) with high range rainbow markers at both ends (GE, Chicago, IL, USA). Following electrophoresis, wet tank transfer was performed and proteins were transferred to a 0.45-µm nitrocellulose membrane and dried for 1 h. Total protein stain was then done with Revert 700 (LI-COR, Lincoln, NE, USA) and the membrane was imaged at 700 nm. The membrane was destained and blocked with Intercept TBS blocking buffer (LI-COR). Primary antibody incubation was performed overnight at 4 °C with anti-RBM3 (Atlas Antibodies AB, Stockholm, Sweden), anti-PDS5A (HPA036661, Atlas Antibodies AB), anti-PRR11 (DCS22, Atlas Antibodies AB), anti-cyclin D3 (DCS22, Cell Signaling, Danvers, MA, USA), or anti-Actin (Cell Signaling, Sigma). The membrane was subsequently washed and incubated for 1 h with secondary antibody IRDye 800CW goat anti-mouse or IRDye 680RD goat anti-rabbit (LI-COR). Once the secondary antibody had been thoroughly rinsed off, near-infrared detection was performed using LI-COR Odyssey Fc imager at 700 or 800 nm. Images were analysed using Image studio software and quantification of relative protein expression, normalised to total protein content, was performed with Empiria studio software (LI-COR).

PRR11 expression in TCGA data set

Clinical data and normalised gene-level expression data from the pancreatic cancer cohort TCGA_PAAD were retrieved from The Cancer Genome Atlas (TCGA) project through the Genomic Data Commons (GDC) (<https://portal.gdc.cancer.gov>, downloaded on 25 May

2021) using the R package TCGAAbiolinks. RNA sequencing data were available for 178 patients. Based on the published curation of the data set by Nicolle *et al* [18], patients with normal pancreas/ampulla/duplicate samples ($n = 12$), non-pancreatic tumour ($n = 4$), non-invasive papillary neoplasms ($n = 2$), tumour origin other than pancreatic ductal adenocarcinoma ($n = 9$), treated with neoadjuvant treatment ($n = 1$), in addition to registered follow-up time of less than 30 days ($n = 5$), were excluded from subsequent analyses. The fragments per kilobase of exon per million mapped reads (FPKM) values were retrieved and the optimal cut-off point for dichotomisation of *PRR11* mRNA expression into low versus high was determined using the survminer package, based on maximally selected rank statistics from the maxstat package.

Kaplan–Meier analysis and log-rank test were applied for evaluation of the prognostic impact of *PRR11* mRNA expression in TCGA data set using the survminer package.

Study cohort

The study cohort is a previously described retrospective consecutive cohort of primary tumours from 175 incident cases of periampullary adenocarcinoma, including pancreatic cancer ($n = 46$) [19]. All patients underwent pancreaticoduodenectomy at the University hospitals of Malmö and Lund in the time span of 1 January 2001 to 31 December 2011. Follow-up started at the date of surgery and ended at death or on 31 March 2017, whichever came first. The Swedish National Civil Register was used to obtain information on vital status. Data on adjuvant treatment were obtained from patient charts. All cases underwent thorough histopathological re-evaluation.

The study received approval from the Ethics Committee of Lund University (reference numbers 2007/445, 2008/35, and 2014/748), through which the committee determined no necessity for informed consent other than the option to withdraw.

Immunohistochemistry and staining evaluation

For immunohistochemical analysis of PDS5A, cyclin D3, and PRR11 expression, 4 µm tissue microarray (TMA) sections were automatically pre-treated using the PT Link system and then stained in an Autostainer Plus (DAKO, Glostrup, Denmark) with the rabbit polyclonal anti-PDS5A antibody HPA036661 (diluted 1:100; Atlas Antibodies AB), the mouse monoclonal anti-cyclin D3 antibody DCS22 (diluted 1:1,600; Cell

Signaling Technology), and the rabbit polyclonal anti-PRR11 antibody HPA023923 (diluted 1:50; Atlas Antibodies AB).

PDS5A and cyclin D3 were mainly expressed in the tumour cell nuclei, and the intensity of expression was denoted as either 0 (negative), 1 (weak), 2 (moderate), or 3 (strong). As PDS5A was found to be expressed in the majority of tumour cells, but with a varying intensity, the fraction of positive nuclear expression was denoted as 1 ($\leq 50\%$) or 2 ($> 50\%$). For cyclin D3, being more sparsely expressed, the absolute fraction of positive cells was estimated. PRR11 was expressed in the cytoplasm and cell membrane, and the intensity of expression was denoted as either 0 (negative), 1 (weak), 2 (moderate), or 3 (strong), and the fraction of positive cells as 0 (0–10%), 1 (11–25%), 2 (26–50%), 3 (51–75%), or 4 (76–100%). The expression of PRR11 and cyclin D3 was annotated by two independent observers (SOH and KJ, the latter is a senior pathologist), and the expression of PDS5A was annotated by three independent observers (SC, VF, and KJ). A joint re-evaluation was then carried out and discrepant cases were discussed to reach consensus.

Immunocytochemistry

TMA's were constructed from the paraffin-embedded cell pellets in the same manner as the tissue samples, as was the subsequent staining of the cells.

Statistical analyses

For changes in mRNA levels after siRNA transfection *in vitro*, Student's *t*-test was performed. Non-parametric Wilcoxon signed-rank, Mann–Whitney *U*, and Kruskal–Wallis tests were applied for analysis of differences in the distribution of PDS5A, cyclin D3, and PRR11 protein expression in primary tumours and lymph node metastases and in relation to clinicopathological parameters. Spearman's rank correlation test was used to investigate the intercorrelations between the expression of investigative markers and RBM3. Two cases who received neoadjuvant therapy were excluded from all statistical analyses, and one additional case was excluded from the survival analyses due to emigration. Kaplan–Meier analysis and the log-rank test were applied to estimate differences in 5-year OS in relation to expression of PDS5A, cyclin D3, and PRR11. The fraction \times intensity across all evaluable cores was calculated for each marker and dichotomised variables of low and high expression were then constructed. For PRR11, classification and regression tree (CRT) analysis established a prognostic

cut-off corresponding to the median value. For PDS5A and cyclin D3, no prognostic cut-off could be established by CRT analysis, and the median value was therefore used in the survival analyses.

Cox regression proportional hazards modelling was applied to estimate hazard ratios for death within 5 years in relation to high and low expression of the three investigated markers. All significant variables from the univariable analysis (PRR11 expression, tumour grade, tumour stage, tumour size, involved lymph nodes, growth in lymph vessels, growth in blood vessels, and perineural growth) were entered into the multivariable analysis using a backwards stepwise model with a probability for stepwise entry at 0.05 and removal at 0.10. Statistical analyses were performed using SPSS Statistics version 25.0 (Armonk, NY, USA) and R version 4.1.0. A *P* value of < 0.05 was considered statistically significant. Graphs were designed using SPSS, R, and GraphPad Prism version 9 (GraphPad Software, LA Jolla, CA, USA).

Results

RBM3-associated cellular processes and genes

As MIAPaCa-2 cells have previously been shown to be the most appropriate model system to study the effects of RBM3 silencing on chemotherapy response [8], this cell line was selected for comparison of the transcriptomes of *siRBM3*-transfected and control cells by next-generation RNA sequencing.

As shown in Figure 1A, MIAPaCa-2 cells with downregulated RBM3 displayed 19 differentially expressed genes (all $p < 0.01$), of which 7 were downregulated (*PDS5A*, *NIPSNAP3A*, *HIF1AN*, *SLC25A44*, *PIGN*, *MORF4L1*, and *AMBRA1*) and 12 were upregulated (*SRPR*, *PRR11*, *BOD1*, *CTD-2510F5.6*, *FAM49B*, *BANF1*, *EPB41L1*, *CIT*, *PIP4K2A*, *SMAP1*, *MCFD2*, and *CCND3*). A summary of the genes and their key functions is provided in supplementary material, Table S1.

As further shown in the volcano plot in Figure 1B, the top downregulated gene was *PDS5A* (cohesin associated factor A), encoding the protein PDS5A involved in sister chromatid cohesion [20], and the top upregulated gene was *CCND3*, encoding the cell cycle regulating protein cyclin D3. Screening in the Human Protein Atlas (HPA) portal (and TCGA) identified three of the genes to be highly prognostic ($p < 0.001$) in pancreatic cancer ($n = 176$) at the mRNA level; *EPB41L1* (shorter OS) encoding erythrocyte membrane protein band 4.1 like 1, an actin-binding protein, *PRR11* (shorter OS) encoding proline rich 11, involved

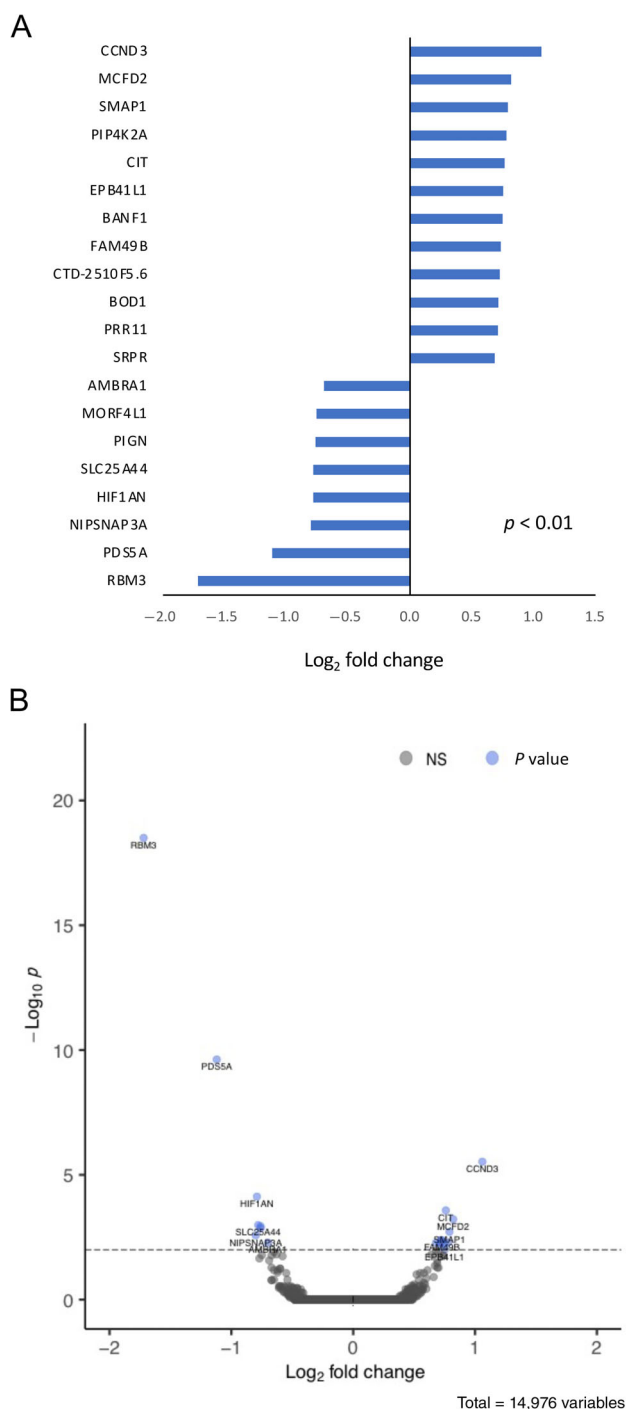


Figure 1. *In vitro* mapping of RBM3-related genes in pancreatic cancer. (A) Bar chart visualising 19 significantly DEGs (adjusted *P* value < 0.01) identified through RNA sequencing of *siRBM3*-transfected and control MIAPaCa-2 cells, of which 12 genes were upregulated and 7 downregulated. (B) Volcano plot of top up- and down-regulated genes showing *PDS5A* as the top down-regulated gene and *CCND3* as the top upregulated gene. NS, non-significant.

in cell cycle progression, and *SLC25A44* (longer OS) encoding solute carrier family 25 member 44, involved in amino acid transport. Given the suggested association of RBM3 with chemosensitivity in pancreatic and other cancers, *PRR11* was selected for further study based on its cellular functions, together with *PDS5A* and *CCND3*, being the top down- and up-regulated genes, respectively.

Effect of RBM3 silencing on expression levels of *PDS5A*, *PRR11*, and cyclin D3 in pancreatic cancer cells *in vitro*

Expression of the selected genes and corresponding proteins was examined in three *siRBM3*-treated pancreatic cancer cell lines, BxPC3, PANC-1, and MIAPaCa-2, and compared with control cells. The results demonstrate that knockdown of RBM3 led to reduced levels of *PDS5A* and increased levels of cyclin D3 and *PRR11*, both at the mRNA and protein levels, in MIAPaCa-2 cells (Figure 2), whereas no significant differences were seen in PANC-1 or BxPC-3 cells, apart from an upregulation of cyclin D3 in the latter. MIAPaCa-2 cells have a higher level of invasiveness and migration than PANC-1 and BPxPC-3 cells, which might explain why significant differences in protein levels were found only in MIAPaCa-2 cells [21].

Protein expression of *PDS5A*, cyclin D3, and *PRR11* in primary tumours and lymph node metastases

Next, the immunohistochemical expression of *PDS5A*, cyclin D3, and *PRR11* was examined in TMAs with matched primary tumours and lymph node metastases from 44 cases of resected pancreatic adenocarcinoma. *PDS5A* expression could be assessed in 43/44 (97.7%) of the primary tumours and in 24/44 (54.5%) of the lymph node metastases; cyclin D3 expression could be assessed in 41/44 (93.2%) of the primary tumours and in 16/44 (36.4%) of the lymph node metastases; and *PRR11* could be assessed in 43/44 (97.7%) of the primary tumours and in 19/44 (43.2%) of the lymph node metastases. Sample immunohistochemical images are demonstrated in Figure 3A. As shown in Figure 3B, the protein expression did not differ significantly between primary tumours and lymph node metastases for *PDS5A* or cyclin D3, whereas significantly lower expression of *PRR11* was found in lymph node metastases compared to primary tumours (*p* = 0.023).

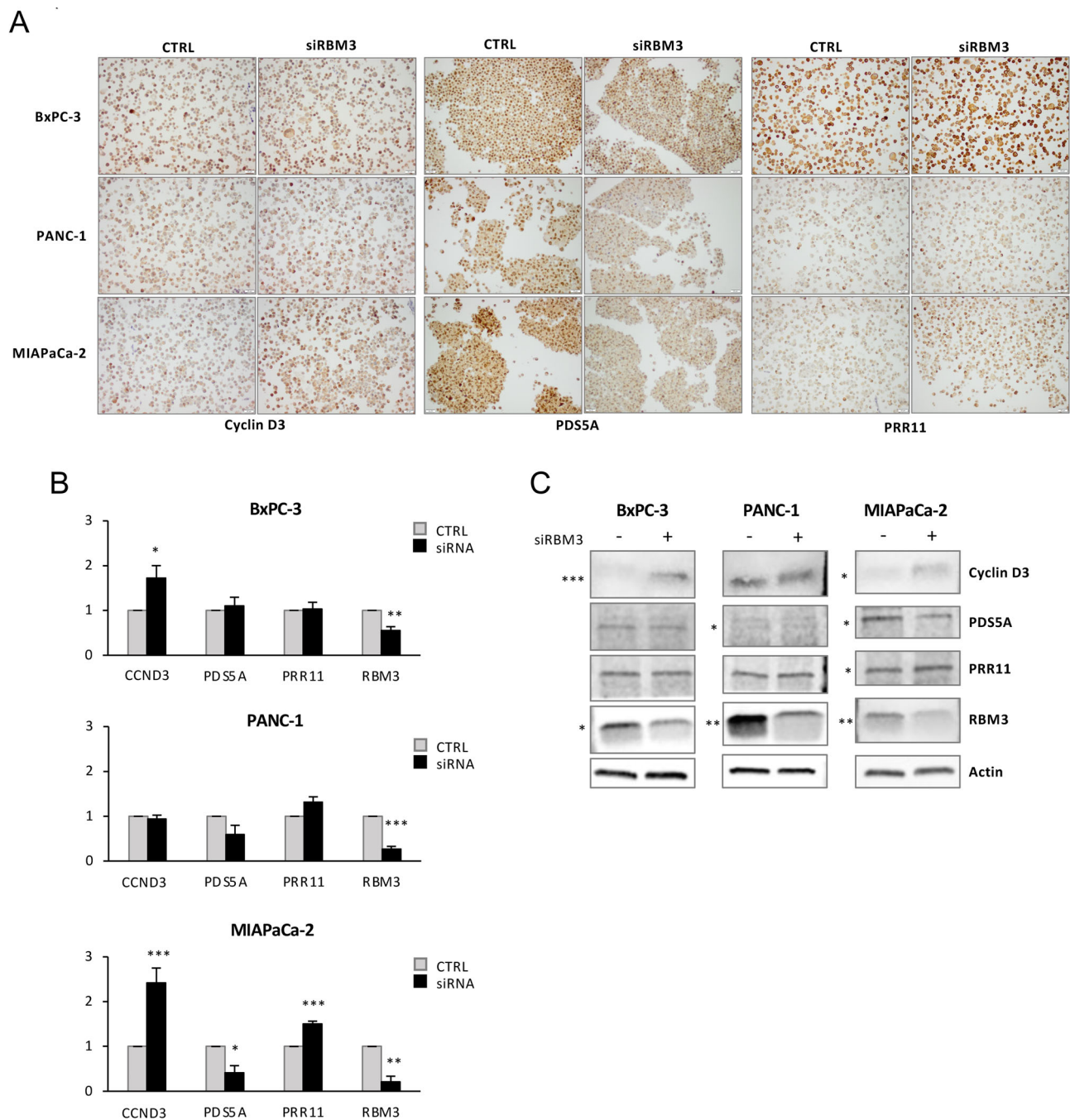


Figure 2. Gene and protein expression of cyclin D3, PDS5A, and PRR11 in three *siRBM3*-treated pancreatic cancer cell lines and controls. (A) Representative images ($\times 20$ objective magnification) of the protein expression of PDS5A, cyclin D3, and PRR11 in BxPC3, PANC-1, and MIAPaCa-2 *siRBM3*-transfected cell lines and controls. (B) Bar charts of the gene expression of *PDS5A*, *CCND3*, and *PRR11* in BxPC3, PANC-1, and MIAPaCa-2 cell lines compared to controls. *** $p < 0.001$, ** $p < 0.01$, * $p < 0.05$. (C) Western blots showing the expression of PDS5A, cyclin D3, and PRR11 in BxPC3, PANC-1, and MIAPaCa-2 cell lines and in controls. *** $p < 0.001$, ** $p < 0.01$, * $p < 0.05$.

Clinicopathological correlates of PDS5A, cyclin D3, and PRR11 protein expression

The distribution of patient and tumour characteristics according to PDS5A, cyclin D3, and PRR11 protein

expression is shown in Table 1. Cyclin D3 expression was associated with lymph node metastases and PDS5A expression was associated with a high tumour grade and involved resection margins.

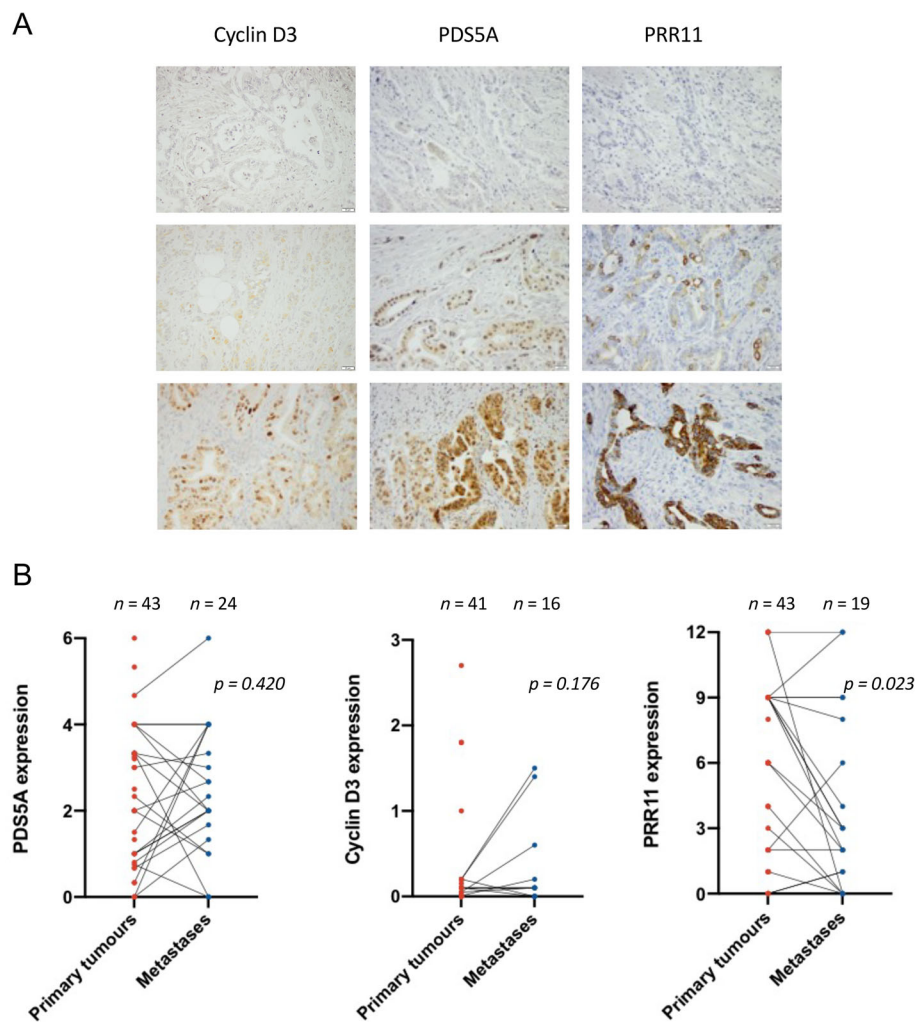


Figure 3. Expression of PRR11 in primary tumours and in lymph node metastases. (A) Sample immunohistochemical images ($\times 20$ objective magnification) of PDS5A, cyclin D3, and PRR11 protein expression in pancreatic cancer. (B) Spaghetti plots visualising the expression of PDS5A, cyclin D3, and PRR11 in paired primary tumours and lymph node metastases.

The intercorrelations of PDS5A, cyclin D3, PRR11, and RBM3 expression are shown in supplementary material, Table S2. The only significant finding was a weakly positive correlation between PDS5A and RBM3 expression ($R = 0.329$, $p = 0.031$).

Prognostic significance of PDS5A, cyclin D3, and PRR11 protein expression

In the in-house cohort, prognostic cut-offs were set at the median for all investigative biomarkers, the median value was 2.0 for PDS5A, 0.01 for cyclin D3, and 5.0 for PRR11. In TCGA, the cut-off for PRR11 was set at the optimal value (1.71 FPKM). Kaplan–Meier analyses showed that both high PRR11 protein expression

(Figure 4A) and high *PRR11* mRNA expression in the curated TCGA data set (Figure 4B) were associated with a significantly shorter 5-year OS. Expression of PDS5A and cyclin D3 did not show any prognostic value in the study cohort (see supplementary material, Figure S1).

As further shown in Table 2, the significant prognostic value of PRR11 was confirmed in univariable Cox regression analysis but did not remain significant in multivariable analysis where only tumour grade and vascular invasion remained independent prognostic factors.

The prognostic value of PDS5A and cyclin D3 did not differ according to adjuvant chemotherapy. In contrast, high PRR11 expression was significantly associated

Table 1. Associations of PDS5A, cyclin D3, and PRR11 expression in primary tumours with clinicopathological parameters.

	<i>n</i>	PDS5A mean, median (SD)	<i>p</i>	<i>n</i>	Cyclin D3 mean, median (SD)	<i>p</i>	<i>n</i>	PRR11 mean, median (SD)	<i>p</i>
Age									
Q1 (38–61)	4	0.58, 0.00 (1.17)	0.11	4	0.04, 0.03 (0.05)	0.62	4	8.75, 9.00 (0.50)	0.27
Q2 (62–67)	13	2.61, 3.25 (1.62)		12	0.27, 0.01 (0.77)		13	4.31, 3.00 (3.82)	
Q3 (68–72)	13	2.38, 3.00 (1.78)		13	0.35, 0.10 (0.65)		13	5.46, 4.00 (4.22)	
Q4 (73–84)	13	2.05, 2.00 (1.65)		12	0.27, 0.01 (0.56)		13	5.38, 6.00 (4.01)	
Gender									
Female	20	2.23, 2.17 (1.69)	0.96	19	0.43, 0.05 (0.80)	0.25	20	5.05, 5.00 (3.47)	0.63
Male	23	2.15, 2.00 (1.69)		22	0.14, 0.01 (0.38)		23	5.70, 6.00 (4.01)	
T stage									
T1–T2	9	1.67, 1.00 (1.34)	0.38	9	0.24, 0.01 (0.59)	0.64	10	6.00, 6.00 (3.62)	0.56
T3–T4	34	2.32, 2.75 (1.71)		32	0.28, 0.03 (0.64)		33	5.21, 6.00 (4.02)	
Lymph node metastasis									
N0	9	2.24, 2.50 (1.92)	0.93	9	0.03, 0.00 (0.07)	0.010	10	5.40, 6.00 (3.98)	0.81
N1	23	2.24, 2.00 (1.68)		21	0.49, 0.00 (0.80)		22	5.05, 5.00 (3.70)	
N2	11	2.02, 2.00 (1.48)		11	0.05, 0.00 (0.08)		11	6.09, 8.00 (4.53)	
Tumour grade									
Low	15	2.52, 3.00 (1.88)	0.47	14	0.17, 0.01 (0.47)	0.29	15	3.73, 3.00 (3.35)	0.043
High	28	2.01, 2.00 (1.52)		27	0.32, 0.05 (0.68)		28	6.29, 6.00 (3.95)	
Tumour size (mm)									
≤20	5	2.17, 2.00 (1.99)	0.86	5	0.02, 0.00 (0.04)	0.07	6	4.00, 6.00 (3.10)	0.30
>20	38	2.19, 2.17 (1.63)		36	0.31, 0.03 (0.65)		37	5.62, 6.00 (4.02)	
Resection margins									
R0	1	1.00, 1.00 (–)	0.57	1	0.20, 0.20 (–)	0.27	2	0.50, 0.50 (0.71)	0.041
R1–2	42	2.21, 2.17 (1.66)		40	0.27, 0.01 (0.63)		41	5.63, 6.00 (3.85)	
Perineural growth									
No	9	1.87, 1.50 (1.82)	0.51	9	0.21, 0.00 (0.60)	0.17	10	4.00, 3.00 (4.19)	0.15
Yes	34	2.27, 2.42 (1.62)		32	0.29, 0.05 (0.63)		33	5.82, 6.00 (3.79)	
Lymphatic invasion									
No	16	2.89, 3.29 (1.79)	0.053	15	0.18, 0.02 (0.47)	0.72	16	4.63, 3.00 (3.81)	0.33
Yes	27	1.77, 1.50 (1.43)		26	0.32, 0.01 (0.70)		27	5.85, 6.00 (3.97)	
Vascular invasion									
No	28	2.17, 2.00 (1.78)	0.93	28	0.25, 0.04 (0.61)	0.79	28	4.75, 4.00 (3.80)	0.16
Yes	15	2.21, 2.33 (1.44)		15	0.28, 0.01 (0.62)		15	6.60, 6.00 (3.96)	
Growth in peripancreatic fat									
No	11	2.02, 2.00 (1.83)	0.71	11	0.20, 0.02 (0.53)	0.78	12	5.17, 6.00 (3.74)	0.83
Yes	32	2.24, 2.17 (1.61)		30	0.30, 0.01 (0.65)		31	5.48, 6.00 (4.03)	

Bold values indicate $p < 0.05$.

with a shorter OS in patients who had received adjuvant chemotherapy, but not in untreated patients. There was, however, no significant treatment interaction between PRR11 and adjuvant treatment (see supplementary material, Table S3).

Discussion

RBM3 has shown promise as a predictive biomarker of improved response to chemotherapy in pancreatic and periampullary adenocarcinoma [8], but the molecular mechanisms underlying these observations have hitherto remained obscure. The results from this study demonstrate links between RBM3 and genes involved in DNA replication, DNA repair, and cell cycle progression

in vitro, further supporting its association to a more chemosensitive phenotype. In terms of prognostication, PRR11 emerged as a top candidate biomarker.

The top downregulated gene *PDS5A* was further confirmed to be linked to RBM3 expression in pancreatic cancer cells *in vitro*, also at the protein level, and weak correlations were found in human tumours. It was only weakly prognostic at the gene expression level in TCGA and not at the protein expression level, neither overall nor in strata according to adjuvant chemotherapy, although high expression was associated with some more favourable clinicopathological factors. *PDS5A* is one of the two cohesion-associated factors; *PDS5A* and *PDS5B*. Cohesin is a chromatin-bound complex that mediates sister chromatid cohesion, thereby facilitating DNA looping and affecting transcriptional activity. A single *PDS5* protein, either *PDS5A* or *PDS5B*, is sufficient for proper

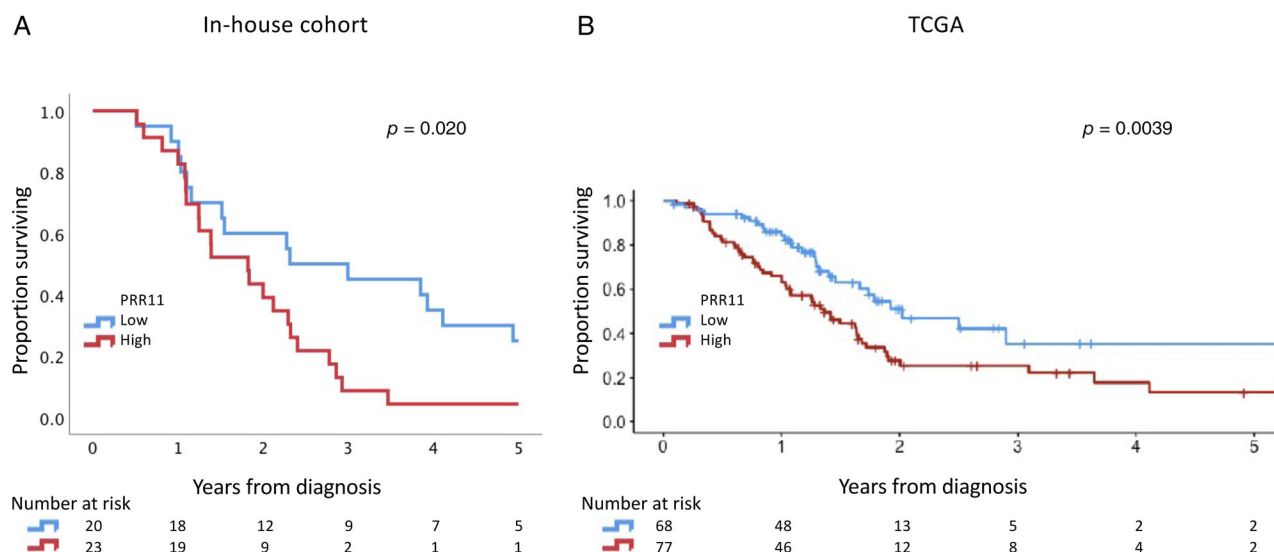


Figure 4. Prognostic significance of PRR11 protein and mRNA expression. Kaplan–Meier analyses of 5-year OS according to (A) PRR11 protein expression in the in-house cohort and (B) *PRR11* mRNA expression in TCGA. *P* values were calculated using the log-rank test.

cohesin dynamics, but simultaneous removal increases binding time of cohesin on chromatin and slows down DNA replication [20]. This is, to the best of our knowledge, the first study to report on the expression and prognostic significance of PDS5A in pancreatic cancer, and its expression in other types of cancer remains largely unknown.

The top upregulated gene *CCND3* and its corresponding protein cyclin D3 were also further confirmed to be linked to RBM3 expression in pancreatic cancer cells *in vitro*, but not in human tumours. It was not prognostic either at the gene or the protein expression level. In normal cells, cyclin D3 has a critical role in cell cycle progression, driving G0/G1 to S-phase. In cancer, including pancreatic adenocarcinoma, cyclin D3 is often overexpressed due to inactivation of the tumour suppressor p16 [22]. Radulovich *et al* demonstrated that downregulation of *CCND3* resulted in decreased proliferation and phosphorylation of Rb in pancreatic cancer cells and that the downregulated genes in *CCND3*-suppressed cells were significantly associated with processes involved in cell cycle progression and programmed cell death [23].

PRR11 was also found to be among the upregulated genes, and the link to RBM3 was further confirmed *in vitro*, but not in human tumours. *PRR11* expression was highly prognostic of poor survival in TCGA, and the prognostic value was further confirmed at the protein level. Of note, PRR11 expression was found to be significantly higher in primary tumours than in lymph node metastases, indicating that a biopsy from the primary tumour would give sufficient prognostic information in unresectable cases; this is in contrast to RBM3 where

higher expression was seen in lymph nodes than in primary tumours [8].

Moreover, high expression of PRR11 was predictive of decreased OS in patients who received adjuvant chemotherapy as opposed to RBM3, where high expression was an independent predictive factor for efficacy of adjuvant chemotherapy [8]. There was, however, no significant treatment interaction between PRR11 and adjuvant chemotherapy, and the potential association of PRR11 with chemoresistance therefore needs validation in a larger cohort.

In TCGA, high RBM3 levels were only weakly significantly associated with shorter survival [8]. Hence, the potential mechanistic relationship between RBM3 and PRR11 in pancreatic cancer also warrants more in-depth study.

The current literature on PRR11 in pancreatic cancer is sparse. Our findings are in line with the study by Tan *et al* including 38 patients, where PRR11 expression was shown to be upregulated in malignant compared to normal pancreatic tissue, and positive expression in pancreatic cancer was associated with shorter survival and clinicopathological factors linked to an aggressive phenotype. Furthermore, knockdown of PRR11 led to reduced migration in pancreatic cancer cells *in vitro* [24]. These findings are in line with studies of PRR11 in other solid carcinomas including ovarian cancer, cholangiocarcinoma, lung cancer, and gastric cancer [25–28].

PRR11 has been shown to promote oncogenesis and cell cycle progression through activation of the phosphatidylinositol-3-kinase (PI3K)/AKT pathway in ovarian and hepatocellular carcinoma [29,30]. Moreover,

Table 2. Univariable and multivariable HRs for death within 5 years according to clinicopathological factors and PRR11 expression.

Factor	N (events)	Univariable HR (95% CI)	Multivariable HR (95% CI)
Age			
Continuous	43 (37)	0.99 (0.94–1.04)	–
Sex			
Female	20 (17)	1.0	–
Male	23 (20)	1.09 (0.57–2.08)	–
Adjuvant chemotherapy			
None	13 (10)	1.0	–
Any	30 (27)	1.33 (0.64–2.76)	–
Tumour stage			
T1–2	10 (6)	1.0	NE
T3–4	33 (31)	3.08 (1.26–7.52)	–
Tumour grade			
Low	15 (9)	1.0	1.0
High	28 (28)	3.43 (1.56–7.56)	2.87 (1.26–6.53)
Tumour size			
Continuous	43 (37)	1.04 (1.01–1.07)	NE
Involved resection margins			
R0	2 (1)	1.0	–
R1–2	41 (36)	3.88 (0.53–28.49)	–
Involved lymph nodes			
N0	10 (7)	1.0	–
N1–2	33 (30)	2.12 (0.92–4.85)	–
Growth in lymph vessels			
Absent	16 (11)	1.0	NE
Present	27 (26)	2.09 (1.02–4.30)	–
Growth in blood vessels			
Absent	28 (22)	1.0	1.0
Present	15 (15)	3.58 (1.69–7.56)	2.81 (1.30–6.07)
Perineural growth			
Absent	10 (6)	1.0	NE
Present	33 (31)	2.60 (1.07–6.31)	–
Growth in peripancreatic fat			
Absent	12 (9)	1.0	–
Present	31 (28)	1.34(0.63–2.86)	–
PRR11 expression*			
Low	20 (15)	1.0	NE
High	23 (22)	2.24 (1.12–4.50)	–

Only cases in which PRR11 could be assessed were included in all analyses and only factors with significant HRs ($p < 0.05$) in the univariable analyses were included in the multivariable analysis. Bold text indicates significant HRs ($p < 0.05$).

HR, hazard ratio; NE, not entered.

*Low expression corresponds to score 0–5, and high expression to score 6–12, corresponding to a cut-off at the median value.

Lee *et al* recently demonstrated that PRR11 enhances PI3K signalling and promotes anti-oestrogen resistance in breast cancer by interacting with the regulatory subunit p85 α [31]. The PI3K/AKT pathway is activated in ~60% of pancreatic cancers and activating mutations in *KRAS*, a hallmark of these tumours, can in turn activate PI3K signalling through the p110 α subunit [32,33]. Given the importance of the PI3K/AKT pathway in many types of solid tumour, there have been vast efforts to introduce PI3K inhibitors as a therapeutic option, with

several ongoing or recently finished phase 1 trials also in pancreatic cancer, but so far toxicity seems to be problematic, especially with oral administration [34–36]. The first drug in clinical use, an inhibitor of the p110 α subunit of PI3K (alpelisib), was however recently approved by the U.S. Food and Drug Administration for the treatment of PI3KCA-mutated, oestrogen receptor positive breast cancer [37]. In light of the above, it could be of value to study the relationship between PRR11 and the PI3K/AKT pathway in more depth in pancreatic cancer too, given the inherent therapeutic resistance of these tumours and the pressing need for improved molecularly guided treatments.

Apart from the genes more closely investigated herein, several other genes within the RBM3-associated transcriptome, *CIT*, *BANF1*, *BOD1*, and *SRPR*, are also involved in chromosome formation and cell cycle progression [38–43]. Moreover, RBM3 is well known to be induced in response to various types of cellular stress [44–48], and several genes with similar functions have been identified: *AMBRA1*, shown to attenuate oncogenesis through autophagy-dependent stress sequestration [49,50]; *SLC25A44*, shown to be upregulated upon cold exposure [51]; and *HIF1AN*, which functions as an oxygen sensor and represses the transcriptional activity of hypoxia-inducible factor 1- α [52]. Other genes, such as *EPB41L1* and *FAM49B*, have been shown to interact with the cytoskeleton and to be involved in proliferation, migration, and metastasis [53–56]. Of note, *EPB41L1* was also found to be highly prognostic at the mRNA level in TCGA. Hence, the RBM3-regulated transcriptome may well harbour additional promising biomarker candidates in pancreatic cancer.

In summary, this study provides further clues about cellular processes and transcriptional partners that may link RBM3 to chemosensitivity in pancreatic cancer, further supporting its potential utility as a predictive biomarker. Moreover, PRR11 is unveiled as a robust prognostic biomarker that merits further attention, possibly also in the context of PI3K signalling and related targeted treatment options.

Acknowledgements

The results are in whole or in part based on data generated by TCGA Research Network: <https://www.cancer.gov/tcga>.

This study was supported by grants from the Swedish Research Council (grant numbers 2015-03598 and 2018-02441), the Swedish Cancer Society (grant no. CAN 2018/418), the Kamprad Family Foundation,

the Mrs Berta Kamprad Foundation, the Faculty of Medicine, Lund University, the Governmental Funding of Clinical Research within the National Health Service (ALF), Skåne University Hospital Funds and Donations, the Irish Cancer Society Collaborative Cancer Research Centre BREAST-PREDICT (CCRC13GAL), the Science Foundation Ireland (SFI) under the Investigator Programme OPTi-PREDICT (15/IA/3104), and the Strategic Research Programme Precision Oncology Ireland (18/SPP/3522).

Author contributions statement

WMG, EK and KJ designed the experiments. SOH, SC, VF, BM, BN, EK and KJ collected the data. JEL performed the histopathological re-evaluation. JEb and JEl collected the clinical data. SOH, SW, SC, VF, BM, BN, EK and KJ analysed the data. SOH, SC, VF, EK and KJ prepared the manuscript. All authors reviewed and approved the manuscript.

References

- Rawla P, Sunkara T, Gaduputi V. Epidemiology of pancreatic cancer: global trends, etiology and risk factors. *World J Oncol* 2019; **10**: 10–27.
- Golan T, Hammel P, Reni M, *et al.* Maintenance olaparib for germline BRCA-mutated metastatic pancreatic cancer. *N Engl J Med* 2019; **381**: 317–327.
- Hilmi M, Bartholin L, Neuzillet C. Immune therapies in pancreatic ductal adenocarcinoma: where are we now? *World J Gastroenterol* 2018; **24**: 2137–2151.
- Aroldi F, Zaniboni A. Immunotherapy for pancreatic cancer: present and future. *Immunotherapy* 2017; **9**: 607–616.
- O'Reilly EM, Oh DY, Dhani N, *et al.* Durvalumab with or without tremelimumab for patients with metastatic pancreatic ductal adenocarcinoma: a phase 2 randomized clinical trial. *JAMA Oncol* 2019; **5**: 1431–1438.
- Marabelle A, Le DT, Ascierto PA, *et al.* Efficacy of pembrolizumab in patients with noncolorectal high microsatellite instability/mismatch repair-deficient cancer: results from the phase II KEYNOTE-158 study. *J Clin Oncol* 2020; **38**: 1–10.
- Saung MT, Zheng L. Current standards of chemotherapy for pancreatic cancer. *Clin Ther* 2017; **39**: 2125–2134.
- Karveli E, Dror LB, Mardinoglu A, *et al.* Translational study reveals a two-faced role of RBM3 in pancreatic cancer and suggests its potential value as a biomarker for improved patient stratification. *Oncotarget* 2018; **9**: 6188–6200.
- Boman K, Segersten U, Ahlgren G, *et al.* Decreased expression of RNA-binding motif protein 3 correlates with tumour progression and poor prognosis in urothelial bladder cancer. *BMC Urol* 2013; **13**: 17.
- Jonsson L, Gaber A, Ulmert D, *et al.* High RBM3 expression in prostate cancer independently predicts a reduced risk of biochemical recurrence and disease progression. *Diagn Pathol* 2011; **6**: 91.
- Salomonsson A, Micke P, Mattsson JSM, *et al.* Comprehensive analysis of RNA binding motif protein 3 (RBM3) in non-small cell lung cancer. *Cancer Med* 2020; **9**: 5609–5619.
- Bronisz A, Rooj AK, Krawczyński K, *et al.* The nuclear DICER-circular RNA complex drives the deregulation of the glioblastoma cell microRNAome. *Sci Adv* 2020; **6**: eabc0221.
- Jonsson L, Bergman J, Nodin B, *et al.* Low RBM3 protein expression correlates with tumour progression and poor prognosis in malignant melanoma: an analysis of 215 cases from the Malmö Diet and Cancer Study. *J Transl Med* 2011; **9**: 114.
- Ehlén A, Brennan DJ, Nodin B, *et al.* Expression of the RNA-binding protein RBM3 is associated with a favourable prognosis and cisplatin sensitivity in epithelial ovarian cancer. *J Transl Med* 2010; **8**: 78.
- Ehlén A, Nodin B, Rexhepaj E, *et al.* RBM3-regulated genes promote DNA integrity and affect clinical outcome in epithelial ovarian cancer. *Transl Oncol* 2011; **4**: 212–221.
- Dobin A, Davis CA, Schlesinger F, *et al.* STAR: ultrafast universal RNA-seq aligner. *Bioinformatics* 2013; **29**: 15–21.
- Love MI, Huber W, Anders S. Moderated estimation of fold change and dispersion for RNA-seq data with DESeq2. *Genome Biol* 2014; **15**: 550.
- Nicolle R, Raffenne J, Paradis V, *et al.* Prognostic biomarkers in pancreatic cancer: avoiding errata when using the TCGA dataset. *Cancers (Basel)* 2019; **11**: 126.
- Elebro J, Jirström K. Use of a standardized diagnostic approach improves the prognostic information of histopathologic factors in pancreatic and periampullary adenocarcinoma. *Diagn Pathol* 2014; **9**: 80.
- Morales C, Ruiz-Torres M, Rodríguez-Acebes S, *et al.* PDS5 proteins are required for proper cohesin dynamics and participate in replication fork protection. *J Biol Chem* 2020; **295**: 146–157.
- Deer EL, González-Hernández J, Coursen JD, *et al.* Phenotype and genotype of pancreatic cancer cell lines. *Pancreas* 2010; **39**: 425–435.
- Ebert MP, Hernberg S, Fei G, *et al.* Induction and expression of cyclin D3 in human pancreatic cancer. *J Cancer Res Clin Oncol* 2001; **127**: 449–454.
- Radulovich N, Pham NA, Strumpf D, *et al.* Differential roles of cyclin D1 and D3 in pancreatic ductal adenocarcinoma. *Mol Cancer* 2010; **9**: 24.
- Tan S, Jiang Z, Hou A, *et al.* Expression of PRR11 protein and its correlation with pancreatic cancer and effect on survival. *Oncol Lett* 2017; **13**: 4117–4122.
- Zhu J, Hu H, Wang J, *et al.* PRR11 overexpression facilitates ovarian carcinoma cell proliferation, migration, and invasion through activation of the PI3K/AKT/beta-catenin pathway. *Cell Physiol Biochem* 2018; **49**: 696–705.
- Chen Y, Cha Z, Fang W, *et al.* The prognostic potential and oncogenic effects of PRR11 expression in hilar cholangiocarcinoma. *Oncotarget* 2015; **6**: 20419–20433.

27. Ji Y, Xie M, Lan H, *et al.* PRR11 is a novel gene implicated in cell cycle progression and lung cancer. *Int J Biochem Cell Biol* 2013; **45**: 645–656.
28. Song Z, Liu W, Xiao Y, *et al.* PRR11 is a prognostic marker and potential oncogene in patients with gastric cancer. *PLoS One* 2015; **10**: e0128943.
29. Wang Y, Zhang Y, Zhang C, *et al.* The gene pair PRR11 and SKA2 shares a NF-Y-regulated bidirectional promoter and contributes to lung cancer development. *Biochim Biophys Acta* 1849; **2015**: 1133–1144.
30. Qiao W, Wang H, Zhang X, *et al.* Proline-rich protein 11 silencing inhibits hepatocellular carcinoma growth and epithelial-mesenchymal transition through beta-catenin signaling. *Gene* 2019; **681**: 7–14.
31. Lee KM, Guerrero-Zotano AL, Servetto A, *et al.* Proline rich 11 (PRR11) overexpression amplifies PI3K signaling and promotes antiestrogen resistance in breast cancer. *Nat Commun* 2020; **11**: 5488.
32. Ebrahimi S, Hosseini M, Shahidsales S, *et al.* Targeting the Akt/PI3K signaling pathway as a potential therapeutic strategy for the treatment of pancreatic cancer. *Curr Med Chem* 2017; **24**: 1321–1331.
33. Hobbs GA, Baker NM, Miermont AM, *et al.* Atypical KRAS(G12R) mutant is impaired in PI3K signaling and macropinocytosis in pancreatic cancer. *Cancer Discov* 2020; **10**: 104–123.
34. Bedard PL, Taberero J, Janku F, *et al.* A phase Ib dose-escalation study of the oral pan-PI3K inhibitor buparlisib (BKM120) in combination with the oral MEK1/2 inhibitor trametinib (GSK1120212) in patients with selected advanced solid tumors. *Clin Cancer Res* 2015; **21**: 730–738.
35. McRee AJ, Sanoff HK, Carlson C, *et al.* A phase I trial of mFOLFOX6 combined with the oral PI3K inhibitor BKM120 in patients with advanced refractory solid tumors. *Invest New Drugs* 2015; **33**: 1225–1231.
36. Patnaik A, Appleman LJ, Tolcher AW, *et al.* First-in-human phase I study of copanlisib (BAY 80-6946), an intravenous pan-class I phosphatidylinositol 3-kinase inhibitor, in patients with advanced solid tumors and non-Hodgkin's lymphomas. *Ann Oncol* 2016; **27**: 1928–1940.
37. André F, Ciruelos EM, Juric D, *et al.* Alpelisib plus fulvestrant for PIK3CA-mutated, hormone receptor-positive, human epidermal growth factor receptor-2-negative advanced breast cancer: final overall survival results from SOLAR-1. *Ann Oncol* 2021; **32**: 208–217.
38. Cong L, Bai Z, Du Y, *et al.* Citron rho-interacting serine/threonine kinase promotes HIF1a-CypA signaling and growth of human pancreatic adenocarcinoma. *Biomed Res Int* 2020; **2020**: 9210891.
39. Halfmann CT, Roux KJ. Barrier-to-autointegration factor: a first responder for repair of nuclear ruptures. *Cell Cycle* 2021; **20**: 647–660.
40. Esmaeeli-Nieh S, Fenckova M, Porter IM, *et al.* BOD1 is required for cognitive function in humans and Drosophila. *PLoS Genet* 2016; **12**: e1006022.
41. Burgess JT, Cheong CM, Suraweera A, *et al.* Barrier-to-autointegration-factor (Banf1) modulates DNA double-strand break repair pathway choice via regulation of DNA-dependent kinase (DNA-PK) activity. *Nucleic Acids Res* 2021; **49**: 3294–3307.
42. Pan D, Du Y, Ren Z, *et al.* Radiation induces premature chromatid separation via the miR-142-3p/Bod1 pathway in carcinoma cells. *Oncotarget* 2016; **7**: 60432–60445.
43. Kim BK, Yoo HI, Choi K, *et al.* Regulation of Srpr expression by miR-330-5p controls proliferation of mouse epidermal keratinocyte. *PLoS One* 2016; **11**: e0164896.
44. Peretti D, Bastide A, Radford H, *et al.* RBM3 mediates structural plasticity and protective effects of cooling in neurodegeneration. *Nature* 2015; **518**: 236–239.
45. Sakurai T, Kashida H, Komeda Y, *et al.* Stress response protein RBM3 promotes the development of colitis-associated cancer. *Inflamm Bowel Dis* 2017; **23**: 57–65.
46. Zhu X, Bühner C, Wellmann S. Cold-inducible proteins CIRP and RBM3, a unique couple with activities far beyond the cold. *Cell Mol Life Sci* 2016; **73**: 3839–3859.
47. Danno S, Nishiyama H, Higashitsuji H, *et al.* Increased transcript level of RBM3, a member of the glycine-rich RNA-binding protein family, in human cells in response to cold stress. *Biochem Biophys Res Commun* 1997; **236**: 804–807.
48. Wellmann S, Bühner C, Moderegger E, *et al.* Oxygen-regulated expression of the RNA-binding proteins RBM3 and CIRP by a HIF-1-independent mechanism. *J Cell Sci* 2004; **117**: 1785–1794.
49. Liu M, Sun T, Li N, *et al.* BRG1 attenuates colonic inflammation and tumorigenesis through autophagy-dependent oxidative stress sequestration. *Nat Commun* 2019; **10**: 4614.
50. Yang Y, Liu L, Li M, *et al.* The chromatin remodeling protein BRG1 links ELOVL3 trans-activation to prostate cancer metastasis. *Biochim Biophys Acta Gene Regul Mech* 1862; **2019**: 834–845.
51. Yoneshiro T, Wang Q, Tajima K, *et al.* BCAA catabolism in brown fat controls energy homeostasis through SLC25A44. *Nature* 2019; **572**: 614–619.
52. Johnatty SE, Tyrer JP, Kar S, *et al.* Genome-wide analysis identifies novel loci associated with ovarian cancer outcomes: findings from the Ovarian Cancer Association Consortium. *Clin Cancer Res* 2015; **21**: 5264–5276.
53. Yang Q, Zhu M, Wang Z, *et al.* 4.1N is involved in a flotillin-1/beta-catenin/Wnt pathway and suppresses cell proliferation and migration in non-small cell lung cancer cell lines. *Tumour Biol* 2016; **37**: 12713–12723.
54. Xi C, Ren C, Hu A, *et al.* Defective expression of Protein 4.1N is correlated to tumor progression, aggressive behaviors and chemotherapy resistance in epithelial ovarian cancer. *Gynecol Oncol* 2013; **131**: 764–771.
55. Zhang Y, Du P, Li Y, *et al.* TASP1 promotes gallbladder cancer cell proliferation and metastasis by up-regulating FAM49B via PI3K/AKT pathway. *Int J Biol Sci* 2020; **16**: 739–751.
56. Yuki KE, Marei H, Fiskin E, *et al.* CYRI/FAM49B negatively regulates RAC1-driven cytoskeletal remodelling and protects against bacterial infection. *Nat Microbiol* 2019; **4**: 1516–1531.
57. Al-Aynati MM, Radulovich N, Ho J, *et al.* Overexpression of G1-S cyclins and cyclin-dependent kinases during multistage human pancreatic duct cell carcinogenesis. *Clin Cancer Res* 2004; **10**: 6598–6605.

58. Zhu M, Zheng C, Wei W, *et al.* Analysis of MCFD2- and LMAN1-deficient mice demonstrates distinct functions in vivo. *Blood Adv* 2018; **2**: 1014–1021.
59. Sangar F, Schreurs AS, Umaña-Díaz C, *et al.* Involvement of small ArfGAP1 (SMAP1), a novel Arf6-specific GTPase-activating protein, in microsatellite instability oncogenesis. *Oncogene* 2014; **33**: 2758–2767.
60. Rameh LE, Tolias KF, Duckworth BC, *et al.* A new pathway for synthesis of phosphatidylinositol-4,5-bisphosphate. *Nature* 1997; **390**: 192–196.
61. Shin YJ, Sa JK, Lee Y, *et al.* PIP4K2A as a negative regulator of PI3K in PTEN-deficient glioblastoma. *J Exp Med* 2019; **216**: 1120–1134.
62. Sumita K, Lo YH, Takeuchi K, *et al.* The lipid kinase PI5P4Kbeta is an intracellular GTP sensor for metabolism and tumorigenesis. *Mol Cell* 2016; **61**: 187–198.
63. Batista PJ, Chang HY. Long noncoding RNAs: cellular address codes in development and disease. *Cell* 2013; **152**: 1298–1307.
64. Buechler C, Bodzioch M, Bared SM, *et al.* Expression pattern and raft association of NIPSNAP3 and NIPSNAP4, highly homologous proteins encoded by genes in close proximity to the ATP-binding cassette transporter A1. *Genomics* 2004; **83**: 1116–1124.
65. Bishop T, Ratcliffe PJ. HIF hydroxylase pathways in cardiovascular physiology and medicine. *Circ Res* 2015; **117**: 65–79.
66. Burrell RA, McClelland SE, Endesfelder D, *et al.* Replication stress links structural and numerical cancer chromosomal instability. *Nature* 2013; **494**: 492–496.
67. Sang Y, Zhang R, Sun L, *et al.* MORF4L1 suppresses cell proliferation, migration and invasion by increasing p21 and E-cadherin expression in nasopharyngeal carcinoma. *Oncol Lett* 2019; **17**: 294–302.

SUPPLEMENTARY MATERIAL ONLINE

Figure S1. Prognostic significance of PDS5A and cyclin D3 expression in pancreatic cancer

Table S1. Summary of the top 19 DEGs and their key functions

Table S2. Correlations between protein expression levels of PDS5A, cyclin D3, PRR11, and RBM3

Table S3. Univariable hazard ratios for death within 5 years according to expression of PDS5A, cyclin D3, and PRR11 in relation to adjuvant chemotherapy